HHS Public Access

Author manuscript

Skeletal Radiol. Author manuscript; available in PMC 2022 February 01.

Published in final edited form as:

Skeletal Radiol. 2021 February ; 50(2): 333–341. doi:10.1007/s00256-020-03558-x.

Mesenchymal chondrosarcoma: Imaging features and clinical findings

Soleen Ghafoor, MD[1,*], **Meera S. Hameed, MD**[2], **William D. Tap, MD**[3], **Sinchun Hwang, MD**[1]

[1]Department of Radiology, Memorial Sloan Kettering Cancer Center, New York, NY, USA

[2]Department of Pathology, Memorial Sloan Kettering Cancer Center, New York, NY, USA

[3]Department of Medicine, Memorial Sloan Kettering Cancer Center and Weill Cornell Medical College, New York, NY, USA

Abstract

Objective.—To describe imaging features and clinical findings of primary mesenchymal chondrosarcoma (MCS) and evaluate for presence of a distinct biphasic pattern on imaging.

Material and methods.—Patients with a pathologic diagnosis of MCS were identified along with imaging of their primary tumor. Size, location, appearance (lytic, sclerotic, or mixed), calcification, cortical destruction, soft tissue extension, contrast enhancement, and radiotracer uptake were recorded. Presence of a biphasic morphology (distinct calcified and noncalcified components) on CT and MRI was assessed. Presence of metastases was documented.

Results.—The study included 23 patients (mean age 28.0±6 years) consisting of 13 skeletal and 10 extraskeletal MCS. Overall mean tumor size was 10.2±7.2 cm, 7.1±7.3 cm in non-metastatic and 13.2±5.9 cm (p=0.004) in metastatic cases. Locations were extremities (n=11), head and neck (n=4), chest wall (n=4), pelvis (n=3), and retroperitoneum (n=1). Skeletal MCS were predominantly lytic (n=8), purely lytic (n=4), or juxtacortical (n=1) and all showed cortical destruction and soft tissue extension. A thick rim enhancement was observed in 5/15 cases on MRI (33%) and 2/4 cases (50%) on CT. Chondroid-type calcification was frequent (n=12). A biphasic morphology on imaging was seen in 39%. Metastases were common (n=12). Common metastatic sites were lungs (75%). Mean SUVmax at PET was 14.3 (5.6–34).

Conclusion.—Skeletal MCS commonly present as lytic lesions with chondroid-type calcifications. In skeletal and primary soft tissue MCS, a biphasic morphology was seen frequently at imaging. Metastases were common at initial presentation and were more commonly seen with larger primary tumors.

[*]**Corresponding Author:** Soleen Ghafoor, MD, Department of Radiology, Memorial Sloan Kettering Cancer Center, 1275 York Avenue, New York, NY 10065, ghafoors@mskcc.org.

Compliance with Ethical Standards

Conflict of interest: The authors declare that they have no conflict of interest.

Ethical approval: All procedures performed in studies involving human participants were in accordance with the ethical standards of the institutional and/or national research committee and with the 1964 Helsinki declaration and its later amendments or comparable ethical standards. This article does not contain any studies with animals performed by any of the authors.

Informed consent: The requirement for informed consent was waived for this study.

Keywords

Mesenchymal Chondrosarcoma; Magnetic Resonance Imaging; Computed Tomography; Biphasic morphology; Imaging

INTRODUCTION

Mesenchymal chondrosarcoma (MCS) is a rare, high-grade malignancy first described in 1959 by the pathologists Lichtenstein and Bernstein [1] as an unusual variant of chondrosarcoma affecting bone and soft tissues. It is a separate entity distinct from conventional or dedifferentiated chondrosarcoma and constitutes fewer than 2% of all chondrosarcomas [2, 3]. Unlike conventional chondrosarcoma, it commonly affects younger patients with a peak incidence during the 3rd decade [3] and is associated with a poorer prognosis and high propensity to metastases, with reported 5-year and 10-year survival rates of 54.6% and 27.3%, respectively [3, 4]. A Surveillance, Epidemiology, and End Results (SEER) database study including 205 patients with MCS evaluating the prognostic determinants for survival in MCS found an overall better prognosis for younger patients and cranial tumors whereas larger tumor size and presence of metastases were poor prognosticators [5].

Microscopically, the characteristic feature is a biphasic pattern made up of solid areas of small round cells, which are referred to as “Ewing-like”, and/or spindle cells around blood vessels, which are referred to as “hemangiopericytic” or “hemangiopericytoma-like”, interspersed with islands of well-differentiated cartilage [6]. Occasionally, in the absence of the characteristic biphasic morphology (for example due to sampling bias on biopsy or only small volume biopsy specimen), the differential diagnosis to other cartilaginous tumors or small round cell tumors may be challenging on pathology. In 2011 a novel fusion transcript called HEY1-NCOA2 was identified as a potential helpful diagnostic tool for MCS that may help in differentiating this entity from other (chondro-)sarcomas in challenging or equivocal cases [7]. This HEY1-NCOA2 fusion gene can be analyzed using fluorescence in situ hybridization (FISH).

Radiographic correlation is an important cornerstone in the evaluation of musculoskeletal tumors, and while imaging does not necessarily obviate the need for tissue sampling, it plays an important role in differential diagnosis, provides guidance in biopsy planning, and is essential for staging.

Due to its rarity, the imaging literature on MCS is scarce and mainly comprised of older or small case series and case reports describing conventional radiographic features. Therefore, the purpose of this study was to describe conventional and cross-sectional imaging features of MCS and to evaluate for the presence of a distinct biphasic pattern on imaging in a series of patients from our institution as a tertiary referral cancer center.

MATERIALS AND METHODS

Patient selection and clinical data

This retrospective study, performed at a tertiary referral cancer center, was approved by the Institutional Review Board with an informed consent waiver. The institutional pathology database was searched for the keywords “mesenchymal” and “chondrosarcoma” in pathology reports dated between January 2009 and August 2019. The resultant list was searched for all cases with a confirmed final pathological diagnosis of MCS and available imaging. Inclusion criteria included a confirmed diagnosis of MCS and available cross-sectional imaging of the primary tumor site. Relevant clinical data from the hospital electronic medical record, including patient demographics and outcomes (development of metastases, mortality) were recorded.

Pathology review

Confirmation of the histologic diagnosis was performed by review of the available slides or pathology reports for each case by an experienced musculoskeletal pathologist (M.H.). The available pathology reports and specimens were either from biopsies (either from the primary tumor or metastatic sites) or from surgical resection. From these, the presence of small round cell (SRC) and/or hemangiopericytoma-like (HPC) as secondary components besides the chondroid tumor component was recorded. In cases where fluorescence in situ hybridization (FISH) for the detection of *HEY1-NCOA2* fusion gene was available, the results were recorded as well. *HEY1-NCOA2*, a recurrent translocation, is diagnostic for MCS and has been reported to be detectable in a significant proportion of specimens (at least 80%) [7, 8].

Imaging studies and image interpretation

For each confirmed case of MCS, all available radiologic examinations (including submitted studies from outside institutions) of the primary tumor site were reviewed on a picture archiving and communication system (PACS). The imaging studies were reviewed by two radiologists with 7 and 15 years of experience who were not blinded to the diagnosis of MCS. Tumors were analyzed for location (if involving the long bones, the location in epi-, meta- or diaphysis was also noted), bone or soft tissue origin, size (longest dimension in any plane; the tumor size measurements were performed on the imaging from the initial presentation of the patients), and morphology if skeletal (purely lytic, mixed lytic and sclerotic, or purely sclerotic). Presence, pattern (defined as rings-and-arcs vs. non rings-and-arcs), location (defined as more peripheral, more central or both/diffuse; if calcifications were seen as exclusively peripheral or exclusively central, then this fulfilled the criteria for the feature of “biphasic morphology” as described below), and extent of calcifications (defined as involving less than one third, between one and two thirds, and more than two thirds of the mass) were recorded. Presence of cortical destruction and soft tissue extension (for skeletal lesions), as well as periosteal reaction (was only assessed if CT or radiographs were available) were assessed. On magnetic resonance imaging (MRI), the signal on T1- (T1W) and T2-weighted (T2W) images (relative to the skeletal muscle) and enhancement characteristics were reviewed. On T2W images, the presence of fluid-signal like T2 hyperintense lobules surrounded by linear or rim-like T2-hypointense signal within the

tumor was assessed, a feature commonly seen in chondroid lesions. On MRI, enhancement was classified into “chondroid-type” or “non chondroid-type” enhancement, the former representing the characteristic peripheral, linear or septal enhancement of chondroid tumors. Furthermore, the presence of a biphasic morphology was noted. For the definition of a biphasic morphology all cases had to have a CT to reliably depict calcifications, if no CT was available for review, the tumors were not assessed for biphasic morphology. The biphasic morphology was defined as presence of two components within the mass with a narrow transition zone, one of which contains clusters of calcifications while the other contains none. The location of the calcifications was not a criterion for the definition of a biphasic pattern, hence whether the calcified component was peripheral or central did not influence the assignment of this feature. For those cases with biphasic morphology, presence of differences in enhancement between the calcified and non-calcified portions were assessed. Metabolic activity of the tumors was assessed by evaluation of increased radiotracer uptake on bone scintigraphy and the maximum standardized uptake value (SUVmax) on positron emission tomography/computed tomography (PET/CT). Further, if metastases were present at baseline imaging or subsequent follow-up imaging, their location was documented.

Statistical analysis

All statistical analyses were performed using SPSS (IBM SPSS Statistics for Windows, Version 21.0. Armonk, NY: IBM Corp.). Continuous variables were expressed as means ± standard deviation (SD) and range (min–max), and categorical variables were expressed as total numbers and percentages. Differences between unpaired data were examined using the Mann–Whitney U test for continuous variables and Fisher’s exact test for categorical variables, respectively. Statistical significance was considered at $p < 0.05$ for all tests.

RESULTS

The search revealed 23 patients with a final pathologic diagnosis of MCS and available imaging of the primary tumor site.

Clinical data

The mean age of the 23 patients (13 female, 10 male) was 28.0 ± 13.8 years. Pain was a presenting symptom in 19 (83%) patients at initial presentation. The mean follow-up time was 42.2 months (range, 0–163 months).

Twelve patients (52%) developed metastases, either pathologically proven or based on the comprehensive review of imaging and clinical follow-up studies. Of those, 6 patients (26%) presented with metastatic disease at initial presentation. Seven patients (30%) died from MCS, all of whom had metastatic disease. Of the patients with primary skeletal MCS (n = 13), 7 patients developed metastatic disease (53.8%) and 4 patients died (31%). Of the patients with primary soft tissue MCS (n = 10), 5 patients developed metastatic disease (50%) and 3 patients died (33.3%).

Metastases were in the lungs (9/12, 75%), bone (7/12, 58%), liver (4/12, 33%), soft tissues (4/12, 33%), pancreas (3/12, 25%), kidneys (2/12, 17%), lymph nodes (2/12, 167%), and adrenals (1/12, 8%).

Pathology review

The pathologic diagnosis was made on the basis of histology and FISH analysis was not required for diagnostic confirmation. The information on the presence of SRC and/or HPC components was not available or could not be derived in 5 patients, since the biopsy sample in those cases was too small to reliably define the whether a SRC or HPC component was the predominant secondary component. Of the remaining 18 patients, both SRC and HPC secondary components were present in 7 patients, and only SRC or HPC secondary components were seen in 9 and 2 patients, respectively. FISH analysis was available in 6 patients, of which 4 were positive for *HEY1-NCOA2* rearrangement (8q21.1 and 8q13.3); one showed *NCOA2* rearrangement using a break apart probe for *NCOA2* and one was negative.

Imaging review

In terms of tumor location, 11 cases were in the extremities (47.8%), 4 were in the chest or chest wall (17.4%), 4 were in the head and neck (17.4%), 3 were in the pelvis (13%), and one was in the retroperitoneal space (4.4%). In terms of bone or soft tissue origin, thirteen cases (56.5%) were primarily located in bone whereas ten cases (43.5%) were extraskeletal and primarily located in soft tissues. Of the 13 skeletal MCS, 7 cases (54%) were in the extremities (Figs. 1–2), with 2 cases in the scapula (Fig. 3) and 5 cases in the long bones. The remaining 6 cases were in following locations: 3 lesions in the bony pelvis, 1 lesion in the rib, 1 lesion in the mandible and 1 lesion in the maxilla. In the long bones, the most common location was the diaphysis (4/5, 80%); one case was in the metaphysis. Of the 10 extraskeletal MCS (Fig. 4), 4 cases were in the extremities (40%), 3 cases were in the chest (either chest wall or mediastinum) (30%), 2 cases were in the head and neck (20%), and 1 case was in the retroperitoneum (10%). Of the extraskeletal MCS that were in the extremities, 3 out of 4 were located in the thigh. There were no differences with regards to age ($p = 0.232$) and sex ($p = 0.552$) distribution between skeletal and extraskeletal MCS.

The mean tumor size measured in the longest dimension was 10.2 ± 7.2 cm (0.6–21.3 cm). The mean tumor size of non-metastatic cases was 7.1 ± 7.3 cm (0.6–25 cm) whereas the mean tumor size of metastatic cases was 13.2 ± 5.9 cm (6.9–23 cm, $p = 0.004$).

In terms of morphology, of the primary skeletal MCS, 8 cases presented as mixed lytic and sclerotic (61.5%), 4 presented as purely lytic (31%), and 1 presented as a juxtacortical mass (8%). No case presented as a purely sclerotic mass.

Calcifications were present in 15 cases (65%) (Figs. 1–4); of those, the predominant pattern was a chondroid type rings-and-arcs pattern of calcifications (12/15, 80%). The location of calcifications was more peripheral in 5 cases (33%), more central in 6 cases (40%), and both peripheral and central in 4 cases (27%). The extent of calcifications was less than one third of the mass in 6 cases (40%), between one third to two thirds in another 6 cases (40%), and more than two thirds of the mass in 3 cases (20%). All 13 skeletal cases showed cortical

destruction and soft tissue extension. Periosteal reaction was present in 6/20 cases (30%, in three cases this feature could not be assessed since no radiograph or CT was available).

MRI was available for review in 17 cases. On MRI, all masses were of hypointense signal on T1W images, except for heterogeneous high T1W signal in parts of one lesion likely corresponding to hemorrhage of recent biopsy. On T2W images, all lesions were hyperintense compared with skeletal muscle; most (15/17, 88%) were heterogeneously hyperintense. The more calcified masses tended to show more heterogeneous appearance than the less calcified masses. Only two cases were relatively homogenous high in signal on T2W images, one lesion was in the mandible and one lesion in the maxilla, both were purely lytic on the corresponding CT and did not show any calcifications. Presence of fluid-signal like T2 hyperintense lobules surrounded by linear or rim-like T2-hypointense signal within the tumor was seen in 6 out of 17 cases on MRI (35%). A contrast-enhanced MRI was available in 15 cases. A chondroid-type enhancement was present in 11 cases (73%). A biphasic morphology on imaging (Figs. 1–4) was present in 7 cases (30%), of which 4 were skeletal and 3 were extraskeletal MCS. In 6 of these cases (86%) the calcified and non-calcified portion showed differences in enhancement, with the calcified portion showing less and heterogeneous enhancement and the non-calcified portion showing more pronounced and homogeneous enhancement (Figs. 1, 3, 4).

Seven cases had available bone scans and all of those showed increased radiotracer uptake at the primary tumor site (BS positive). FDG PET/CT (Figs. 1–3) was available in six cases and all of them showed increased uptake of the tumor with a mean SUVmax of 13.4 (range, 5.6–34). Of those cases with a biphasic morphology on CT, four had a BS, PET/CT or both (n=1 PET/CT, n=1 BS, n=2 PET/CT and BS). In two of these cases, the calcified portions of the mass showed less uptake or were more photopenic compared to the non-calcified portions of the mass (Figs. 3 – 4), while in the other two cases the uptake was relatively diffuse without a difference between the calcified and non-calcified component (Fig. 1).

DISCUSSION

This is to date one of the largest case series focused on cross-sectional imaging features of both skeletal and extraskeletal (i.e. soft tissue) MCS. MCS can either arise from the bone or soft tissues and the proportion of primary soft tissue MCS are reported in a broad range of 10 – 60% [3–5, 9–12]. In our cohort, 43.5% of the cases primarily arose in the soft tissues. Our main findings are that both skeletal and extraskeletal MCS commonly presented as large masses (>10 cm) and commonly presented with chondroid-type calcifications (80%). Skeletal MCS were lytic or mixed lytic and sclerotic lesions that always presented with cortical destruction and varying degrees of soft tissue extension indicating an aggressive behavior. A distinct biphasic morphology, defined as the presence of a calcified and non-calcified component within a mass separated by a sharp transition zone, could be seen in 30% of cases. Chondroid-type enhancement, defined as septal and peripheral enhancement, was commonly seen in these tumors (in 73%). On MRI, the presence of T2-hyperintense lobules, a feature commonly seen in chondroid lesions, could be seen in 35%. Clinically, patients tended to be young and development of metastases was common, of which the most

common sites were the lungs and bones (78% and 58%), but uncommon sites like pancreas and kidneys were also seen.

Mesenchymal chondrosarcoma is a distinct and rare type of high-grade chondrosarcoma consisting of a microscopically biphasic histology with subtypes of either predominantly small round cell components (sometimes also referred to as “Ewing-like”) and/or hemangiopericytoma-like components in the background of island of well-differentiated chondroid tissue. The published literature on MCS is limited to case reports [13–17] and case series [2, 11, 18, 19] and only a few incorporated imaging findings.

Imaging plays an important role in management and accurate diagnosis of MCS. The presence of the biphasic morphology may hinder accurate diagnosis in the setting of non-image guided biopsies or inadvertent selective biopsy of only one component of the two components, resulting in inconclusive histologic diagnosis or erroneous diagnosis of other tumors with small round blue cell components such as Ewing’s sarcoma, small cell osteosarcoma, and dedifferentiated chondrosarcoma depending on the biopsied component [20]. A further complicating factor related to sampling is that the proportion of the chondroid and mesenchymal components may vary widely among cases [8].

A biphasic morphology with the presence of distinct tumor components on imaging, one calcified and one non-calcified, was seen in 30% in our cohort. In this study we have tried to propose a clear definition of a biphasic morphology that requires the presence of separate calcified and non-calcified portions within a tumor. This feature as such has not yet been studied as such in prior studies. However, in a study by Hashimoto et al [19] including 10 cases of extraskeletal MCS the authors described four cases (40%) where there was a clear demarcation between the calcified and non-calcified tumor components (two cases had central calcifications with a periphery of non-calcified tumor and two cases had eccentric peripheral calcifications with a non-calcified center) indicating a presence of biphasic morphology. If present, it is an important feature to include in the radiology report and may help in biopsy planning. Similar findings were also reported by Shapeero et al. [21], albeit they did not as clearly define biphasic morphology as two distinct calcified and non-calcified tumor components.

In our cohort, we found that both skeletal and extraskeletal MCS commonly present as large masses (mean size 10.0 cm, range, 0.6–21.3 cm) with calcifications (65%) that were commonly chondroid-type (80%). All skeletal MCS presented as aggressive bone lesions, namely mixed lytic and sclerotic or lytic lesions with cortical destruction and varying degrees of soft tissue extension. In 30% of cases a periosteal reaction was present. These findings are in line with previously published studies confirming the generally aggressive type of bone involvement in skeletal MCS that presents as moth-eaten or permeative-type of bone destruction [3, 11, 22].

MR signal characteristics of MCS were non-specific with low signal on T1W images and heterogeneously hyperintense signal on T2W, the degree of which depended on the amount and distribution of low T2 signal calcifications, which is in line with previously published reports [23, 24]. In our study, we assessed for the presence of T2-hyperintense or fluid-

signal like lobules with peripheral T2-hypointensity similar to features characteristically seen in chondroid lesions and found it in 35% in our cohort. Interestingly, although we observed a chondroid rings-and-arcs pattern in 80% of the lesions with calcifications, this did not seem to directly translate into a characteristic chondroid appearance on T2-weighted MRI. We did not find other studies describing the presence of a characteristic chondroid appearance of this tumor on T2W MRI. However, most other studies described an overall hyperintense T2 signal of the tumor compared with skeletal muscle with varying degrees of heterogeneity depending on the extent of calcifications [19, 21].

A chondroid type of enhancement, namely a septal and or peripheral linear enhancement, was seen in 73% of cases. Of note, this feature was assessed as present even if only parts of the tumor showed this pattern of enhancement and in most cases, there were coexistent areas of non-chondroid and more heterogeneous or diffuse enhancement too. Further, in 86% of the cases with biphasic morphology, the two components of the masses showed differences in enhancement, with the non-calcified portion showing more homogenous and pronounced enhancement. In the study by Hashimoto et al [19] the enhancement was described as heterogeneous involving the calcified and non-calcified tumor components in the two available cases. Another two cases by Shapeero et al [21] showed enhancement on MRI with foci of non-enhancement corresponding to calcifications, the pattern of enhancement however was not described in more detail. Other authors have described pattern of enhancement as variable, ranging from homogeneous to heterogeneous [23].

On bone scintigraphy all tumors showed increased radiotracer uptake and were hypermetabolic on PET/CT with a mean SUVmax of 13.4 and a wide range of 5.6 – 34. Few other case reports have described PET/CT findings in MCS with reported SUVmax values ranging from 4.1 to 20 [25–28]. The presence of hypermetabolic activity and radiotracer uptake may be expected given that mesenchymal chondrosarcomas tend to be high grade tumors. Moreover, another study investigating 29 benign and malignant chondroid lesions with ^{18}FDG-PET scans including one case of mesenchymal chondrosarcoma noted that FDG uptake increased with tumor grade [28].

The patients in our series tended to be young with a mean age of 28.0 ± 13.8 years. Half of the patients (52%) developed metastatic disease with a mortality of 30%. The frequency of metastases and mortality rate was similar for soft tissue MCS (50% and 33.3%, respectively) and skeletal MCS (53.8% and 31%, respectively).These findings regarding clinical course are largely in line with previously published data [4, 9, 11, 19]. The most common site of metastases were the lungs in 75% of cases, however unusual sites of metastases were seen in 42% of cases (kidneys and pancreas). Unusual sites of metastases were also reported in other studies and case reports [29–32]. Furthermore, there are case reports of primary extraskeletal mesenchymal chondrosarcoma arising from unusual sites such as the kidneys, heart and lung [33–36].

There are several limitations of our study. First, the relatively small number of patients from a single institution may limit the generalizability of the findings; however, this is relative given the extremely rare nature of this type of chondrosarcoma. Another limitation is the retrospective nature of the study, which we think is again is difficult to address given the

rarity of this entity. The imaging studies available for review included studies performed at outside facilities; CT and MRI techniques were thus not standardized, potentially limiting assessment of signal characteristics. The number of cases was insufficient to allow meaningful assessment of inter-reader variability which further was not the primary objective of this study. Further, the fact that a proportion of the cases had only pathology specimen derived from biopsies with the inherent risk of sampling bias and that FISH analysis had not been performed on all cases precluded valid correlations between imaging and pathologic features (i.e. correlation of biphasic pattern on imaging with biphasic pattern on pathology). Lastly, we did not compare the presence of the here described imaging features and the biphasic morphology to other types of chondrosarcoma. The discriminatory value of these imaging findings in clinical practice needs will need to be addressed in future studies with a larger number of different types of chondrosarcomas.

In conclusion, MCS is a rare high-grade variant of chondrosarcoma that affects young patients, with high propensity to metastasize to lungs and bone but also uncommon locations. It commonly presents as a large deep soft tissue mass or aggressive lytic bone lesion with chondroid-type calcifications. Metastases are more common at initial presentation, especially with larger tumors (>10 cm). On MRI, the masses were heterogeneously hyperintense and classic “chondroid” T2-hyperintense lobules were only seen in 35% of cases. A biphasic morphology consisting of a distinct calcified and non-calcified tumor component can be seen in one third of the cases, may be a helpful diagnostic clue and should be noted in order to guide biopsy planning and subsequent management strategies since small biopsy samples may confound the diagnosis by under-sampling of the histologic biphasic component.

Acknowledgements

The authors would like to thank Joanne Chin for her editorial support on this manuscript.

Funding: This study was supported in part through the National Institutes of Health/National Cancer Institute Cancer Center Support Grant P30 CA008748.

References

1. Lichtenstein L, Bernstein D. Unusual benign and malignant chondroid tumors of bone. A survey of some mesenchymal cartilage tumors and malignant chondroblastic tumors, including a few multicentric ones, as well as many atypical benign chondroblastomas and chondromyxoid fibromas. Cancer. 1959; 12(6):1142–1157. [PubMed: 14416919]
2. Bertoni F, Picci P, Bacchini P, Capanna R, Innao V, Bacci G, et al. Mesenchymal chondrosarcoma of bone and soft tissues. Cancer. 1983; 52(3):533–541. [PubMed: 6861090]
3. Nakashima Y, Unni KK, Shives TC, Swee RG, Dahlin DC. Mesenchymal chondrosarcoma of bone and soft tissue. A review of 111 cases. Cancer. 1986; 57(12):2444–2453. [PubMed: 3697943]
4. Cesari M, Bertoni F, Bacchini P, Mercuri M, Palmerini E, Ferrari S. Mesenchymal chondrosarcoma. An analysis of patients treated at a single institution. Tumori. 2007; 93(5):423–427. [PubMed: 18038872]
5. Schneiderman BA, Kliethermes SA, Nystrom LM. Survival in Mesenchymal Chondrosarcoma Varies Based on Age and Tumor Location: A Survival Analysis of the SEER Database. Clin Orthop Relat Res. 2017; 475(3):799–805. [PubMed: 26975384]
6. Hameed M. Small round cell tumors of bone. Arch Pathol Lab Med. 2007; 131(2):192–204. [PubMed: 17284103]

7. Wang L, Motoi T, Khanin R, Olshen A, Mertens F, Bridge J, et al. Identification of a novel, recurrent HEY1-NCOA2 fusion in mesenchymal chondrosarcoma based on a genome-wide screen of exon-level expression data. Genes, Chromosomes and Cancer. 2012; 51(2):127–139. [PubMed: 22034177]
8. Nakayama R, Miura Y, Ogino J, Susa M, Watanabe I, Horiuchi K, et al. Detection of HEY1-NCOA2 fusion by fluorescence in-situ hybridization in formalin-fixed paraffin-embedded tissues as a possible diagnostic tool for mesenchymal chondrosarcoma. Pathology International. 2012; 62(12):823–826. [PubMed: 23252872]
9. Huvos AG, Rosen G, Dabska M, Marcove RC. Mesenchymal chondrosarcoma a clinicopathologic analysis of 35 patients with emphasis on treatment. Cancer. 1983; 51(7):1230–1237. [PubMed: 6825046]
10. Dobin SM, Donner LR, Speights VO Jr. Mesenchymal chondrosarcoma. A cytogenetic, immunohistochemical and ultrastructural study. Cancer Genet Cytogenet. 1995; 83(1):56–60. [PubMed: 7656206]
11. Shakked Rachel J., Geller David S., Gorlick Richard, Dorfman Howard D. Mesenchymal Chondrosarcoma: Clinicopathologic Study of 20 Cases. Archives of Pathology & Laboratory Medicine. 2012; 136(1):61–75. [PubMed: 22208489]
12. Bishop MW, Somerville JM, Bahrami A, Kaste SC, Interiano RB, Wu J, et al. Mesenchymal Chondrosarcoma in Children and Young Adults: A Single Institution Retrospective Review. Sarcoma. 2015; 2015:608279.
13. Chen S, Wang Y, Su G, Chen B, Lin D. Primary intraspinal dumbbell-shaped mesenchymal chondrosarcoma with massive calcifications: a case report and review of the literature. World J Surg Oncol. 2016; 14(1):203. [PubMed: 27487949]
14. Kumar M, Suresh K, Patil M, Pramod R, Yusuf R, Bilahari N. Mesenchymal chondrosarcoma of posterior maxilla: report of a case with brief literature review. Ann Med Health Sci Res. 2014; 4(Suppl 1):S49–52. [PubMed: 25031908]
15. Singh P, Singh A, Saxena S, Singh S. Mesenchymal chondrosarcoma of mandible: A rare case report and review. J Oral Maxillofac Pathol. 2014; 18(Suppl 1):S167–170. [PubMed: 25364172]
16. Taori K, Patil P, Attarde V, Chandanshive S, Rangankar V, Rewatkar N. Primary retroperitoneal extraskeletal mesenchymal chondrosarcoma: a computed tomography diagnosis. Br J Radiol. 2007; 80(959):e268–270. [PubMed: 17989325]
17. White DW, Ly JQ, Beall DP, McMillan MD, McDermott JH. Extraskeletal mesenchymal chondrosarcoma: case report. Clin Imaging. 2003; 27(3):187–190. [PubMed: 12727057]
18. Dantonello TM, Int-Veen C, Leuschner I, Schuck A, Furtwaengler R, Claviez A, et al. Mesenchymal chondrosarcoma of soft tissues and bone in children, adolescents, and young adults: experiences of the CWS and COSS study groups. Cancer. 2008; 112(11):2424–2431. [PubMed: 18438777]
19. Hashimoto N, Ueda T, Joyama S, Araki N, Beppu Y, Tatezaki S, et al. Extraskeletal mesenchymal chondrosarcoma: an imaging review of ten new patients. Skeletal Radiol. 2005; 34(12):785–792. [PubMed: 16211384]
20. Lee AF, Hayes MM, LeBrun D, Espinosa I, Nielsen GP, Rosenberg AE, et al. FLI-1 Distinguishes Ewing Sarcoma From Small Cell Osteosarcoma and Mesenchymal Chondrosarcoma. Applied Immunohistochemistry & Molecular Morphology. 2011; 19(3):233–238. [PubMed: 21084965]
21. Shapeero LG, Vanel D, Couanet D, Contesso G, Ackerman LV. Extraskeletal mesenchymal chondrosarcoma. Radiology. 1993; 186(3):819–826. [PubMed: 8430193]
22. Salvador AH, Beabout JW, Dahlin DC. Mesenchymal chondrosarcoma—observations on 30 new cases. Cancer. 1971; 28(3):605–615. [PubMed: 5096926]
23. Murphey MD, Walker EA, Wilson AJ, Kransdorf MJ, Temple HT, Gannon FH. From the Archives of the AFIP. RadioGraphics. 2003; 23(5):1245–1278. [PubMed: 12975513]
24. Shapeero LG, Vanel D, Couanet D, Contesso G, Ackerman LV. Extraskeletal mesenchymal chondrosarcoma. Radiology. 1993; 186(3):819–826. [PubMed: 8430193]
25. Tsuchiya M, Masui T, Otsuki Y, Sakahara H. 18F-FDG PET/CT Findings of Mesenchymal Chondrosarcoma of the Orbit. Clin Nucl Med. 2018; 43(2):e43–e45. [PubMed: 29215408]

26. Lee E, Lee HY, Choe G, Kim KJ, Lee WW, Kim SE. Extraskeletal intraspinal mesenchymal chondrosarcoma; 18F-FDG PET/CT finding. Clin Nucl Med. 2014; 39(1):e64–66. [PubMed: 23877507]
27. Uppaluri SA, Yin LH, Goh GH. Maxillary mesenchymal chondrosarcoma presenting with epistaxis in a child. J Radiol Case Rep. 2015; 9(8):33–38. [PubMed: 26629302]
28. Feldman F, Heertum RV, Saxena C, Parisien M. 18FDG-PET applications for cartilage neoplasms. Skeletal Radiology. 2005; 34(7):367–374. [PubMed: 15937711]
29. Yamamoto H, Watanabe K, Nagata M, Honda I, Watanabe S, Soda H, et al. Surgical treatment for pancreatic metastasis from soft-tissue sarcoma: report of two cases. Am J Clin Oncol. 2001; 24(2):198–200. [PubMed: 11319298]
30. Tsukamoto S, Honoki K, Kido A, Fujii H, Enomoto Y, Ohbayashi C, et al. Chemotherapy Improved Prognosis of Mesenchymal Chondrosarcoma with Rare Metastasis to the Pancreas. Case Reports in Oncological Medicine. 2014; 2014:249757.
31. Paasch C, De Santo G, Boettge KR, Strik MW. Mesenchymal chondrosarcoma metastasising to the pancreas. BMJ Case Reports. 2018; 11(1):e226369.
32. Chatzipantelis P, Karvouni E, Fragoulidis GP, Voros D, Pafiti A. Clinicopathologic features of two rare cases of mesenchymal metastatic tumors in the pancreas: review of the literature. Pancreas. 2006; 33(3):301–303. [PubMed: 17003653]
33. Huang H-Y, Hsieh M-J, Chen W-J, Ko S-F, Yang B-Y, Huang S-C. Primary mesenchymal chondrosarcoma of the lung. The Annals of Thoracic Surgery. 2002; 73(6):1960–1962. [PubMed: 12078803]
34. Hsing CT, Oh SY, Lee S, Kwon HC, Kim SH, Park TH, et al. Extraskeletal mesenchymal chondrosarcoma of the heart responded to systemic chemotherapy: a case report. Cancer Res Treat. 2007; 39(3):131–133. [PubMed: 19746223]
35. Salehipour M, Hosseinzadeh M, Sisakhti AM, Parvin VAM, Sadraei A, Adib A. Renal Extra Skeletal Mesenchymal Chondrosarcoma: A Case Report. Urology Case Reports. 2017; 12:23–25. [PubMed: 28271053]
36. Gherman V, Tomuleasa C, Bungardean C, Crisan N, Ona V-D, Feciche B, et al. Management of renal extraskeletal mesenchymal chondrosarcoma. BMC Surgery. 2014; 14(1):107. [PubMed: 25511186]

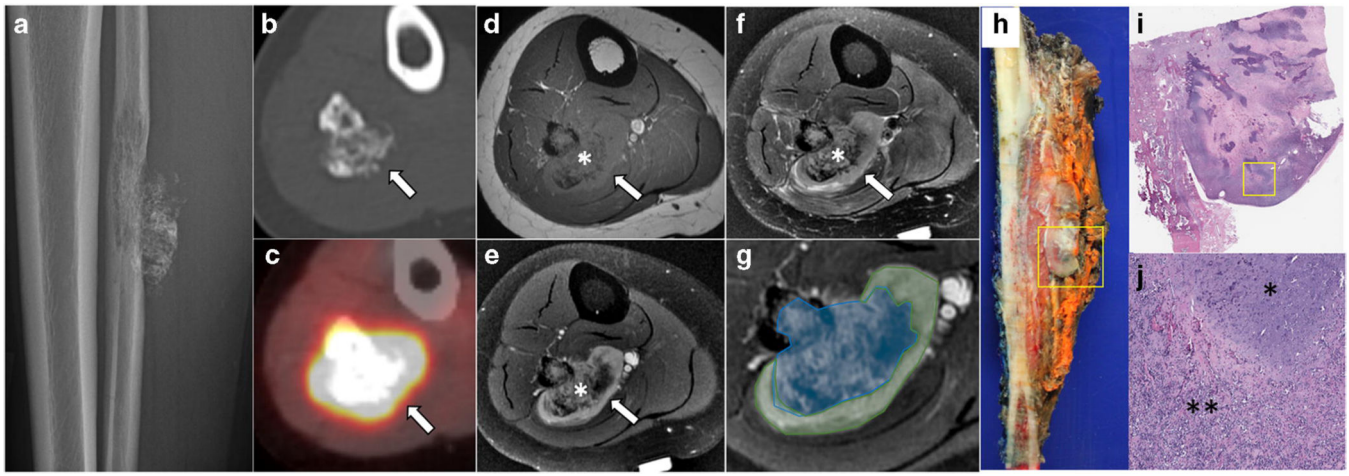

Fig. 1 –.

Primary skeletal mesenchymal chondrosarcoma of the fibula in a 24-year-old woman. Lateral radiograph (a) shows a permeative lytic lesion in the midshaft of the fibula with cortical destruction, soft tissue extension, and calcifications. Axial CT (b) again demonstrating the soft tissue component containing calcifications (arrow). On PET/CT (c), the lesion is avid with a SUVmax of 15.8 (arrow). Axial T1-weighted (d), fat-suppressed T2-weighted (e), and T1 fat-suppressed post-contrast (f and g) reveal a biphasic pattern of the mass with a distinct calcified (asterisk in d–f, blue shaded area in g) and non-calcified component (long arrow in d–f, green shaded area in g). Gross specimen (h) shows the mass in the fibula with soft tissue component (square) with corresponding low- (i) and high-power (j) field microscopic images revealing the biphasic pattern comprised of blue hyaline cartilage (asterisk in j) contrasting with solid proliferation of spindled tumor cells (double asterisk in j).

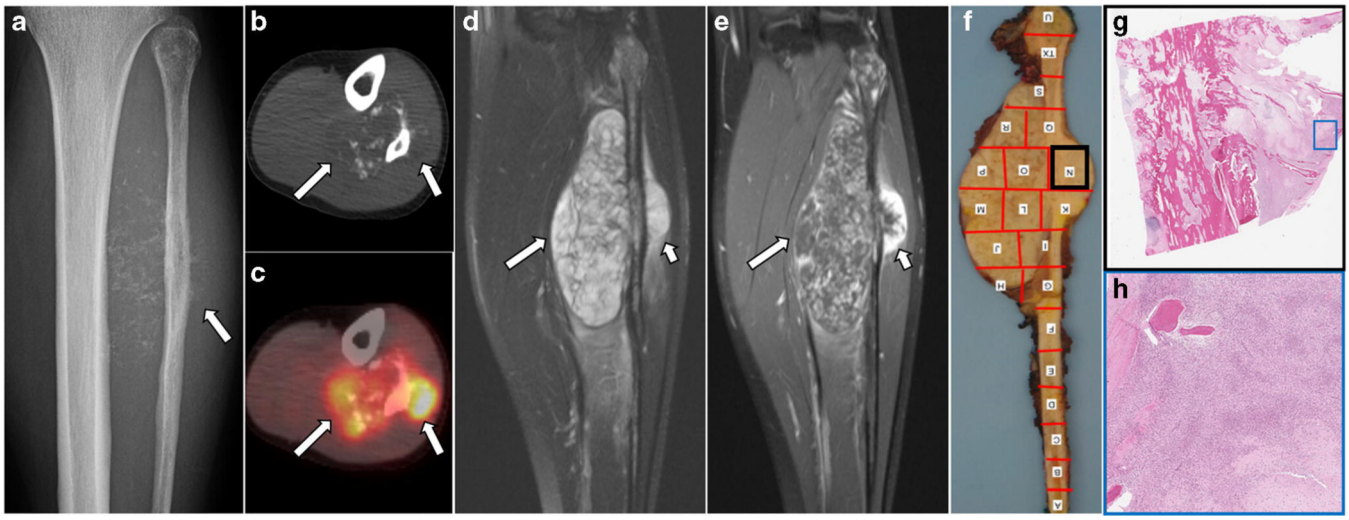

Fig. 2.

Primary skeletal mesenchymal chondrosarcoma of the fibula in a 22-year old woman. Radiograph (a) shows ill-defined permeative destructive lesion in the proximal to mid fibular shaft with extraosseous soft extension containing chondroid-type calcifications. A lateral component (arrow in a) is associated with a sunburst type periosteal reaction. Axial non-contrast CT (b) and axial fused PET-CT (c) images better depict chondroid calcifications clustered in relatively non-FDG-avid medial soft tissue component (long arrows in b and c) while the FDG-avid lateral peripheral soft tissue component is less calcified on the corresponding PET/CT (long arrows in b and c). Coronal fat-suppressed T2-weighted (d) and post-contrast T1-weighted images (e) show two differential components; whereas the medial portion appears more heterogeneous on fat-suppressed T2-weighted images (long arrow in d) with thin linear and curvilinear enhancement on post-contrast T1-weighted (long arrow in e), the lateral component is more homogenous on fat-suppressed T2-weighted images (short arrow in d) with a thick rim of contrast enhancement (short arrow in e). The corresponding gross specimen (f) with bone mapping shows this lateral portion (black box) which consists of small round cells microscopically (g – low power view and h - medium power view).

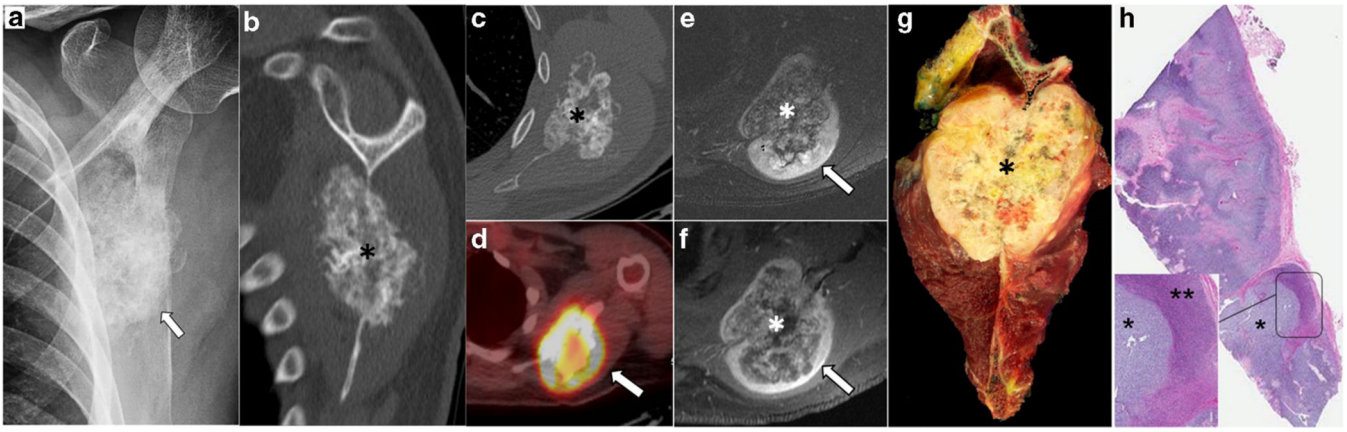

Fig. 3.

Primary skeletal mesenchymal chondrosarcoma with biphasic pattern in a 24-year-old man. Left scapular radiograph (a) showing relatively densely calcified lesion overlying the left scapula (arrow). Coronal reformatted (b) and axial (c) CT better depict the origin of the mass centered in the scapular body with dense calcification (asterisk in b and c). On PET/CT (d), the mass is avid with a preferential uptake in the periphery of the lesion (SUVmax 8.6, arrow in d). On axial fat-suppressed T2-weighted (e) and post-contrast T1-weighted (f) images, the mass is seen to have a biphasic morphology with a lower signal central component (asterisk in e and f, corresponding to calcified portion on CT and less FDG-avid portion on PET/CT) and a higher signal, solid enhancing portion in the periphery (arrows in e and f, corresponding to a non-calcified rind of tissue which showed higher uptake on PET/CT). Gross pathology specimen (g) of the resected scapular mass (asterisk). The corresponding microscopic findings (h - low power view) show a tumor with biphasic morphology with two relatively distinct components comprised of hyaline cartilage (asterisk in magnified view of h) and the presence of small round cells (double asterisk in magnified view of h).

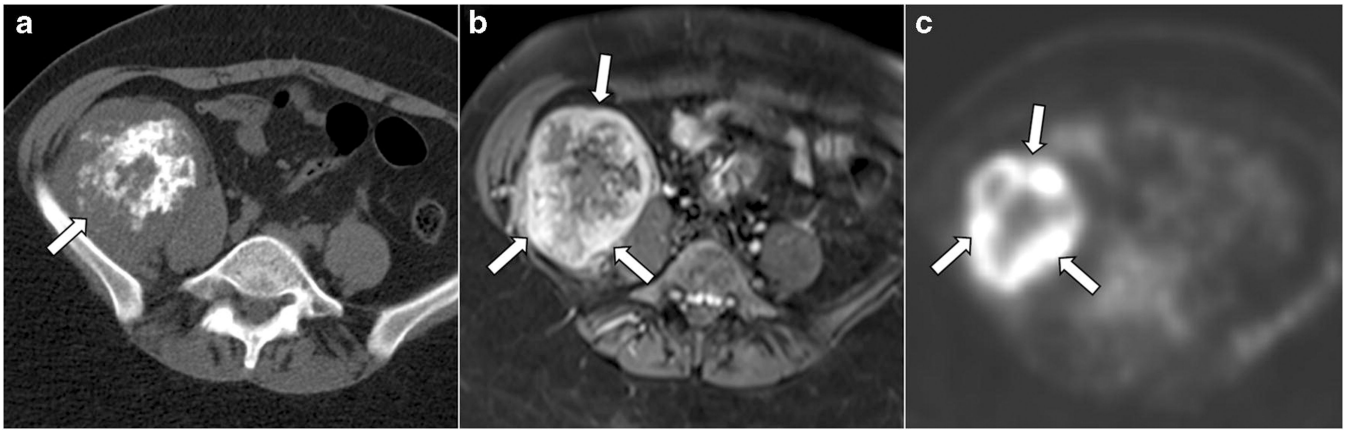

Fig. 4.

Primary soft tissue retroperitoneal mesenchymal chondrosarcoma with biphasic pattern in a 34-year-old woman. Axial non-contrast CT (a) shows a mass (arrow in a) in the right iliac fossa inseparable from the right iliacus muscle and a biphasic imaging appearance with a distinct calcified (central) and non-calcified (periphery) components. Post-contrast axial T1-weighted fat-suppressed image (b) shows a thick enhancing peripheral rim (arrows in b) corresponding to the non-calcified components on the CT. The mass is avid on axial PET (c) with a mean SUVmax of 13.6. Note that the periphery of the mass, corresponding to the non-calcified components, shows the highest uptake on PET (arrows in c).

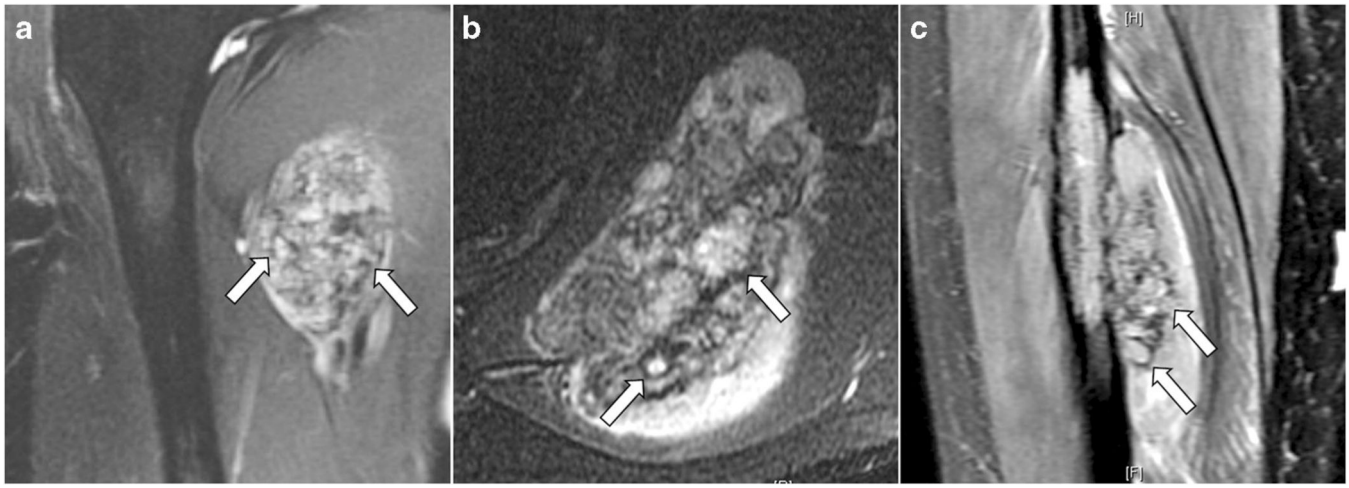

Fig. 5.

Three examples of “chondroid matrix” on fat-suppressed T2-weighted MRI depicted by the presence of T2-hyperintense lobules (arrows) surrounded by peripheral T2-hypointense signal in a case of extraskeletal mesenchymal chondrosarcoma in the upper medial thigh (a), a primary skeletal lesion in the scapular body (b), and another primary skeletal lesion in the mid-diaphysis of the fibula (c)